Battery Charger for Electric Vehicles based on a Wireless Power Transmission

Paolo Germano, *Senior Member*, *IEEE*, and Yves Perriard, *Senior Member*, *IEEE*
(Invited)

***Abstract*—In this paper, the case of a battery charger for electric vehicles based on a wireless power transmission is addressed. The specificity of every stage of the overall system is presented. Based on calculated and measured results, relevant capacitive compensations of the transformer and models are suggested and discussed in order to best match the operating mode and aiming at simplifying as much as possible the control and the electronics of the charger.**

***Index Terms*—Battery charge, battery model, control strategy, converter topologies, electric vehicle, non-linear load, shielding, wireless power transmission.**

I. Introduction

NOWDAYS devices needing electrical power are often supplied through batteries. They have become light, highly capacitive at an affordable price. By using batteries, a high level of freedom of movement is reached. Among a huge variety of devices, one can quote: everyday appliance, gardening tools, toys and vehicles, flying in the air or running on roads. To recharge batteries, Inductive Coupled Power Transmission (ICPT), also known as Wireless Power Transmission (WPT) brings lots of advantages in terms of simplicity of use (no handling, no plugging), safety for users (no electrical hazard, no sparkle risks) or reliability (no wear, no mechanical fitting) [1], [2]. Therefore, such recharging systems spread quickly.

In some cases, space requirements, simplicity, compatibility and price criteria lead to minimize the power chain. Contactless charging may bring solutions that perfectly fit such requirements.

For an ICPT battery recharging system, a usual conversion-chain is depicted in Fig. 1. It is composed of a power source and a DC/AC converter supplying an air transformer and a tuning capacitor, located on the ground part. The mobile part is composed of the secondary winding of the transformer, its tuning capacitor and a rectifier that supplies the battery system. A feedback link allows monitoring the battery state.

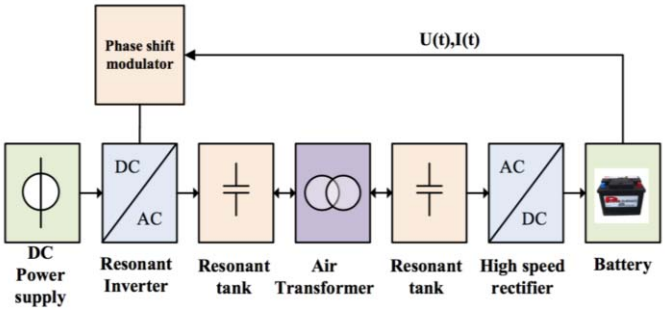

Fig. 1. Typical wireless conversion-chain.

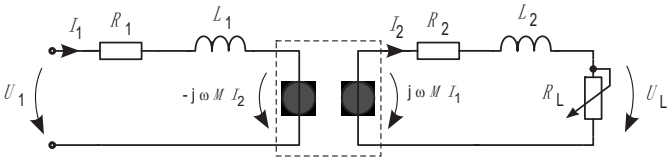

Fig. 2. Transformer's EEC.

The corresponding equivalent electrical circuit (EEC) of the transformer is presented in Fig.2. No tuning capacitors are shown and an equivalent load resistance RL replaces the rectifier and battery system.

II. Specificities Linked To Electric Vehicles

In the case of a battery charger for electric vehicles based on an ICPT, the designer has to face particular points brought by the system:

- Battery management;
- Battery model;
- Ease of control and inter-operability;
- Shielding.

As all of these features are key-points of the conversion chain, they will influence the choices that will be made in the developments.

A. Battery Management

According to [3] and [4], modern rechargeable batteries must have their charge cycle complying with the typical cycle presented in Fig. 3. One can distinguish a first period where the

Paolo Germano, is with Integrated Actuators Laboratory (LAI), École Polytechnique Fédérale de Lausanne (EPFL), Rue de la Maladière 71 B, P.O. Box 526 CH-2002 NEUCHATEL-SWITZERLAND (e-mail: paolo.germano@epfl.ch), http://lai.epfl.ch

Yves Perriard is with Integrated Actuators Laboratory (LAI), École Polytechnique Fédérale de Lausanne (EPFL), Rue de la Maladière 71 B, P.O. Box 526 CH-2002 NEUCHATEL-SWITZERLAND, (e-mail: yves.perriard@epfl.ch) , http://lai.epfl.ch

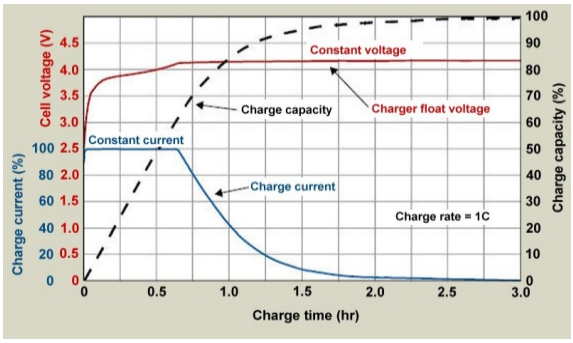

Fig. 3. Typical battery recharge cycle.

charge is performed in a "constant current" mode and the following one in a "constant voltage" mode.

Such specifications require a DC/DC converter that is able to manage the aforementioned modes. Moreover, its power capability must be in the order of magnitude of the supply, i.e., in the present context, nearly the power furnished by the primary resonant inverter.

B. Battery Model

When considering the EEC of an inductive transformer, the output load is assumed to be a linear variable resistance, as shown in Fig. 2. To recharge the battery, the high frequency AC voltage has to be rectified, introducing non-linear elements into the circuit (0).

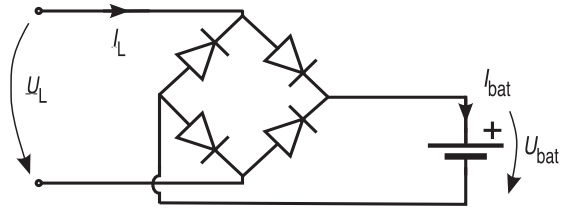

Fig. 4. Current rectifier–Connecting the transformer to the battery.

According to [4] and [11], the rectifier and the battery are replaced by an equivalent resistance RL, in order to still be able to use the conventional models of the transformer.

For a current rectifier, the relation between U_{bat} (battery voltage) and U_L (transformer output voltage) is given by (1).

$$U_L = \frac{2\sqrt{2}}{\pi} U_{bat} \tag{1}$$

Solving the equations of the compensated transformer, the equivalent load resistance R_L is given by (2).

One can see that R_L is dependent of the charge state of the battery U_L.

$$R_L = \frac{\omega_0 M U_L}{U_{in}} \tag{2}$$

C. Ease of control and inter-operability

Most designers aim at providing a transformer's capacitive compensation to mainly optimize the PWT efficiency. This means satisfying equations (3) and (4).

$$\frac{\partial P}{\partial C_2} = 0 \quad \text{and} \quad \mathrm{Im}(\underline{Z}_t(C_1)) = 0 \tag{3)(4}$$

The solution, presented in [11], leads to maximize the efficiency and allows reducing the size of the wires. The reactive part of the whole transformer is cancelled. Capacitance C_2 is set to maximize the power sent to the load and then, capacitance C_1 is set to cancel the reactance of the overall transformer.

However, ICPT may see their operating conditions vary widely since coreless transformers are used [5]. Coupling between primary and secondary is dependent of the vehicle mechanical dimensions, relative positioning and burden. Electrical load is different between an empty or a fully recharged battery. Furthermore, as many companies may be present in the field, inter-operability may be a success key. Therefore, conventional compensation, as described here above, will probably reach limitations.

D. Shielding

By nature, as leakage flux is dominant in air transformers, inductive power transmission systems are strong magnetic field emitting devices. Therefore, to comply with national regulations [8], carmakers have to equip their charging devices with a specific shielding [9].

A typical shielding structure, including ferrite plates, aluminum shorted turns and an iron plate (car body) is illustrated in Fig. 5.

The optimization proposed in [10] emphasis the fact that the shielding dimensions (X_i) are greatly dependent on the size of the vehicle and on the admissible field strength at the border of the car (line $\mathscr{L}_1$).

Obviously, due to the diversity of carmakers, no standardized shielding can be found. Therefore, a robust control unit of the inverter is needed to adapt to variations of load (iron losses) and inductances (coupling) encountered.

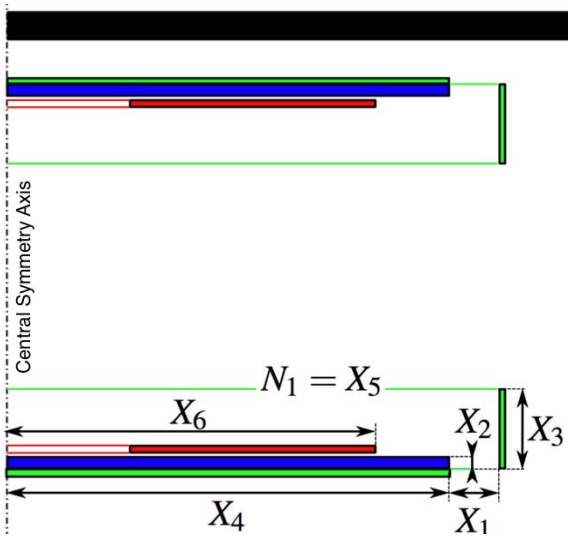

Fig. 5. Shielding optimization.

III. Compensation Topologies

As air transformers are used at high frequency due to their low mutual coupling, primary and secondary impedances are very high. Therefore, compensation capacitors are used both at the primary side (C_1) and at the secondary side (C_2). Even with a very low coupling factor, efficiency can be kept at very high levels.

Well-known and widely used compensation topologies are shown in Fig. 6.

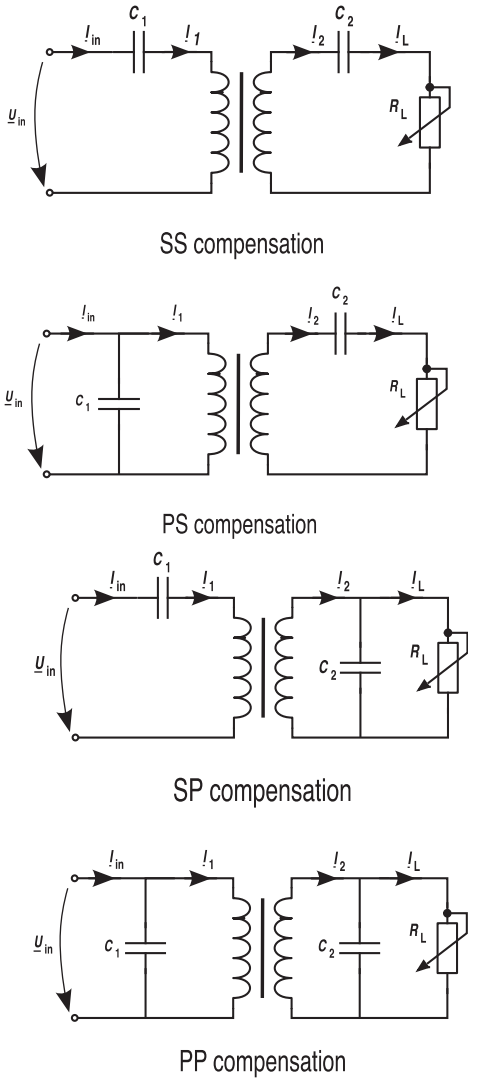

Fig. 6. Common compensastion topologies.

To calculate the primary and the secondary compensation capacitances, for every case [11], the first step consists in calculating the secondary impedance $\underline{Z}_2$, reflect it to the primary, leading to $\underline{Z}_r$, and then calculate the primary impedance $\underline{Z}_1$. This methodology is called "Efficiency-oriented compensation (EOC)".

Then, all electrical quantities are determined from these calculated impedances:

$$\underline{U}_1 = \underline{Z}_1 \cdot \underline{I}_1 \quad \text{and} \quad \underline{I}_2 = j\frac{\omega M \underline{I}_1}{\underline{Z}_2} \qquad (5)(6)$$

According to [13], optimal compensation capacitances are calculated using (3) and (4) and are shown on TABLE I.

TABLE I
Compensation Capacitances (EOC)

Topology	Control-oriented
SS	$C_2 = \frac{1}{\omega_0^2 L_2} \quad C_1 = \frac{1}{\omega_0^2 L_1}$
SP	$C_2 = \frac{1}{\omega_0^2 L_2} \quad C_1 = \frac{L_2}{\left(L_1 L_2 - M^2\right)\omega_0^2}$
PS	$C_2 = \frac{1}{\omega_0^2 L_2} \quad C_1 = \frac{L_1 R_L^2}{L_1^2 R_L^2 \omega_0^2 + M^4 \omega_0^2}$
PP	$C_2 = \frac{1}{\omega_0^2 L_2^2} \quad C_1 = \frac{L_2^3\left(L_1 L_2 - M^2\right)}{M^4 R_L^2 + L_2^2\left(M^2 - L_1 L_2\right)^2 \omega_0^2}$

Based on calculations made in [11], and assuming coil's resistances are near to zero, the load characteristics for the two primary serial compensations can be established as stated in (7) and (8). For the serial-serial (SS) topology:

$$I_{L_{R_1=0,R_2=0}} = \frac{U_1}{M\omega_0} \qquad (7)$$

This result shows that a serial-serial topology based resonant inverter behaves as a **current source**.

And for the serial-parallel (SP) topology:

$$U_L = \frac{L_2}{M} \cdot U_1 \qquad (8)$$

This result shows that a serial-parallel topology based resonant inverter behaves as a **voltage source**.

Measurements have been performed on an air transformer (Fig. 7) having the following size:

- Primary coil - 600 x 600 mm2 (dotted lines);
- Secondary coil - 400 x 400 mm2;
- Air-gap - 260 mm.

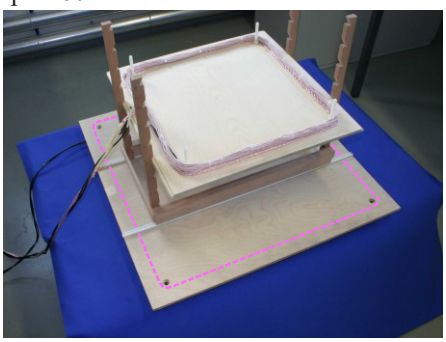

Fig. 7. Air transformer prototype of the studied WPT system.

Results of performed measurements are shown in Fig. 8 and Fig. 9. As stated in [11], Model 1 and Model 2 represent two different theoretical calculations.

Redrawing and merging these two characteristics into a single graph (Fig. 10) may highlight the two topologies behavior. Slope of the ideal voltage source (resp. current source) characteristic should be zero (resp. infinite) but as curves represent real operating conditions with non-ideal components,

ideal characteristic cannot be reached.

Theoretical and measured voltage-current characteristic slope (or $\Delta U/\Delta I$) values are shown in TABLE II.

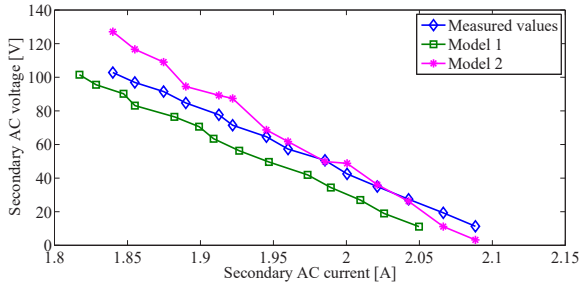

Fig. 8. SS-compensated transformer's voltage-current (V-I) characteritic.

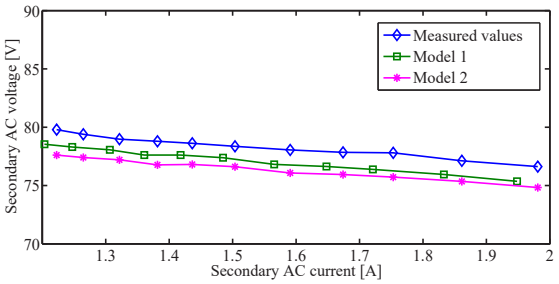

Fig. 9. SP-compensated transformer's voltage-current (V-I) characteritic.

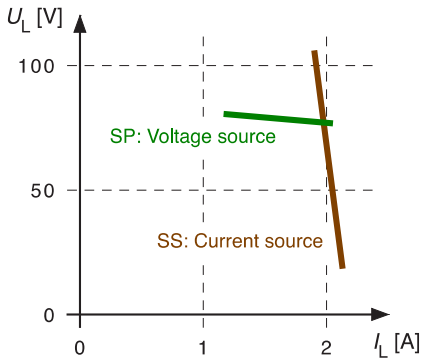

Fig. 10. SS- and SP-compensated transformer load characteristics.

TABLE II
REAL SOURCE CHARACTERISTICS

Parameter	Topology	Theoretical value	Measured value
$\frac{\Delta U}{\Delta I}[\Omega]$	SS	-488	-400
$\frac{\Delta U}{\Delta I}[\Omega]$	SP	-4.24	-4.39

Featuring such values, the transformer can be considered as a good voltage or current source.

Therefore, one can come to the major conclusion that sequentially combining these two topologies using relays at the secondary part (SW1 to SW3), the inverter can be simply turned into a current source or a voltage source, fulfilling the requirements for a battery charger (Section II.A). The main advantage of this solution, called "Dual Topology", is to greatly simplify the embedded electronics as proposed in [11] and illustrated in Fig. 11.

Switches set in the displayed position lead to a SS topology and in the "dotted position" to a SP topology.

Transition from SS topology to SP topology must be done with power turned off as an inductor is opened and a capacitor shorted. Furthermore, the use of the SS topology implies to carefully control the primary side when reducing the load or removing the secondary part due to its instability.

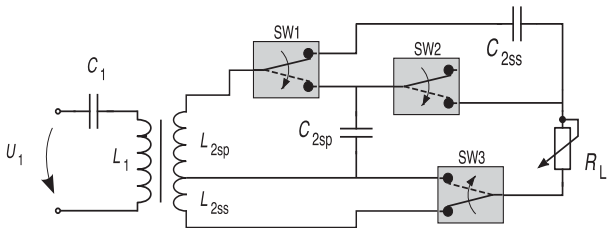

Fig. 11. Transformer with secondary switching features (Patented).

IV. CONTROL-ORIENTED COMPENSATION

A capacitance calculation method is proposed in [12]. Unlike the method presented in II.C, it is an interesting way to compensate the reactive part of the transformer by solving (9) to (12), and therefore finding the compensation capacitances independently from the transformer's parameters.

$$\frac{\partial C_i}{\partial R_L}=0 \quad \text{and} \quad \frac{\partial C_i}{\partial M}=0 \qquad (9)(10)$$

$$\frac{\partial^2 \eta}{\partial C_i^2}=0 \quad \text{and} \quad \mathrm{Im}(\underline{Z}_t)=0 \qquad (11)(12)$$

This methodology is mostly relevant for cases where the design of the primary part (inverter) and the one of the secondary part (battery charger) are not provided by the same developers. This leads to a higher inter-operability between the components, as partial derivatives of C_i are minimized.

Developers of the primary side may propose solutions that are less sensitive to secondary components or variations that may appear such as aging or regular parameter variations. This methodology is called "Control-oriented compensation (COC)".

Results are presented in TABLE III. No differences appear for the two primary serial compensation topologies. On the contrary, regarding the primary parallel compensations, one can notice that for PS compensation, C_1 expression no longer depends on the load resistance R_L (battery state effect, see II.B, Eq. (2)), nor on the mutual inductance M (coupling effect) and C_2 is less coupling-dependent.

For the PP compensation, only C_1 is load-independent and coupling less dependent.

The following example, extracted from [12], shows the robustness of the method: The WPT is first tuned using the EOC and then the COC methods, while having a medium load (R_L = 30 Ω). For both cases, the load is then increased to a higher load (R_L = 4 Ω). On Fig. 12, one can see the new waveform of the inverter voltage in both EOC and COC cases.

The COC method leads to no change of the waveform that remains a rectified sine wave (no detuning).

As main criterion of the COC is no longer efficiency, the transformer's primary current increases in an expected manner. The phenomenon is true only for low load resistance values (high power). It is illustrated on Fig. 13 calculation results.

Although the COC method tends to increase the primary current at high load, the output power is also increased (Fig. 14) resulting in a limited loss of overall efficiency (Fig. 15).

A key point is to verify that the efficiency is not decreased using the methodology.

TABLE III
COMPENSATION CAPACITANCES (COC)

Topology	Control-oriented
SS	$C_2 = \frac{1}{\omega_0^2 L_2}\ C_1 = \frac{1}{\omega_0^2 L_1}$
SP	$C_2 = \frac{1}{\omega_0^2 L_2}\ C_1 = \frac{L_2}{\left(L_1 L_2 - M^2\right)\omega_0^2}$
PS	$C_2 = \frac{L_1}{\left(L_1 L_2 - M^2\right)\omega_0^2}\ C_1 = \frac{1}{\omega_0^2 L_1}$
PP	$C_2 = \frac{1}{\omega_0^2 L_2}\ C_1 = \frac{L_2}{\left(L_1 L_2 - M^2\right)\omega_0^2}$

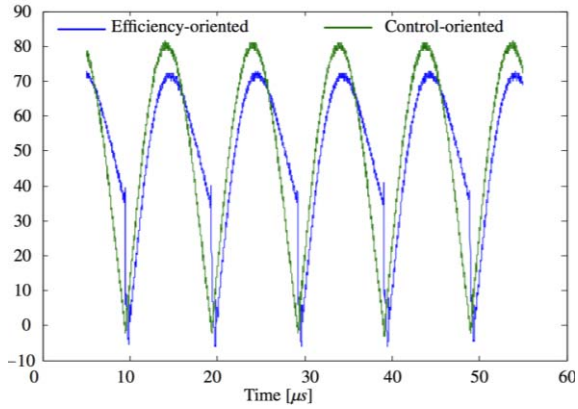

Fig. 12. Inverter voltage comparision – EOC vs. COC

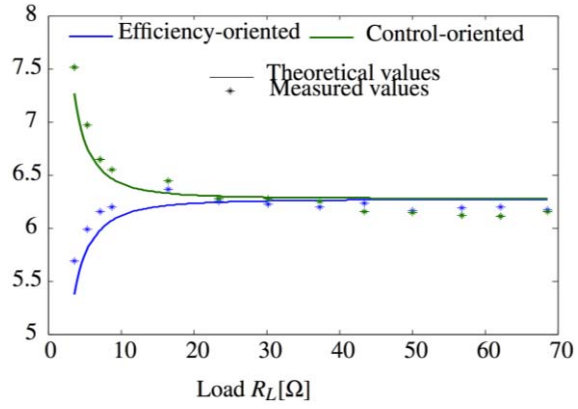

Fig. 13. Inverter primary current comparision – EOC vs. COC

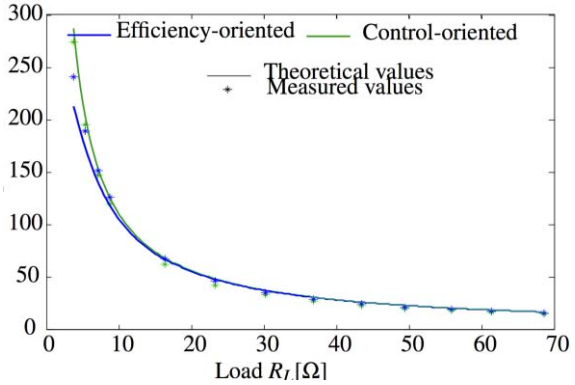

Fig. 14. EOC vs. COC – Output power comparision.

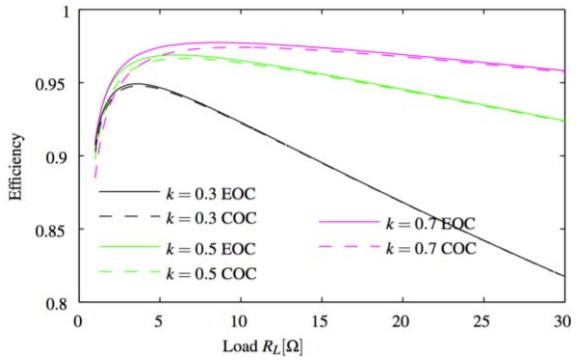

Fig. 15. Efficiency comparison between EOC and COC vs. load – Coupling factor *k* set as parameter.

One can notice a loss of a few percent with the COC method but only for a high load current and in case of relative high coupling. Electric vehicle inductive charging devices often feature high air-gaps and therefore low coupling factors leading to very low efficiency drop.

In addition to the benefits the method can bring to criteria of Section II.C, it may be interesting also for those of Section II.D as shielding may vary from different carmakers and from EMC local regulations. Indeed, shielding directly affects the internal parameters of the transformer: Eddy currents affect the mutual inductance M on the one hand. Iron losses change the load resistance R_L on the other hand. Having a device insensitive to such variations may bring other benefits.

V. CONCLUSION

Focusing on electric vehicle inductive battery chargers, one can see that several requirements have to be met. Battery charge modes, robustness of control and electromagnetic compliance are the most important ones but when considering economic aspects, simplicity and reliability become important too. Furthermore, if inter-operability, or standardization, may be reached, chances for ICPT systems being quickly spread in industry, public and private transportation vehicles are real.

This paper aims at presenting developed principles tending to bring relevant solutions. Two major innovations are brought. The “Dual-topology” ICPT allows to greatly simplify the embedded electronics by suppressing a DC/DC converter. The “Control-Oriented Compensation” enhances the functioning by avoiding dependencies to the system parameters.

Depending on its own requirements, the reader will be able to make the right choices for the development of a wireless battery charger.

REFERENCES

[1] G. Covic and J. Boys, "Modern trends in inductive power transfer for transportation applications," *Emerging and Selected Topics in Power Electronics, IEEE Journal of*, vol. 1, no. 1, pp. 28-41, 2013.

[2] J. Sallan, J.Villa, A.Llombart and J.Sanz, "Optimal design of icpt systems applied to electric vehicle battery charge," *Industrial Electronics, IEEE Transactions on*, vol. 56, no. 6, pp. 2140–2149, 2009.

[3] www.batteryuniversity.com.

[4] C. S. Wang, O. H. Stielau and G. A. Covic, *"*Design consideration for a contactless electric vehicle battery charger*"*, *IEEE Trans. Ind. Electron*, vol. 52, no. 5, pp. 1308, U˝1313, Oct, 2005.

[5] J.L. Villa, J. Sallán, J.F.S. Osorio and A. Llombart, *"*High- Misalignment Tolerant Compensation Topology for ICPT Systems,*"* *IEEE Transactions on Ind. Electronics*, vol. 59, pp. 945-951, Aug. 2011.

[6] C. Auvigne, P. Germano, Y. Civet and Y. Perriard, "Design considerations for a contactless battery charger", *16th European Conference on Power Electronics and Applications (EPE'14 - ECCE Europe)*, Page 1-7, 2014, DOI: 10.1109/EPE.2014.6910704.

[7] R.L. Steigerwald, "A comparison of half-bridge resonant converter topologies," *IEEE Transactions on Power Electronics*, vol. 3, no. 2, pp. 174-182, April 1988.

[8] ICNIRP, "ICNIRP Guidelines for Limiting Exposure to Time-varying Electric, Magnetic and Electromagnetic Elds (up to 300 GHz)," 1998.

[9] F. Nakao, Y. Matsuo, M. Kitaoka, and H. Sakamoto, "Ferrite core couplers for inductive chargers," in *Power Conversion Conference, 2002. PCC Osaka 2002. Proceedings of the*, vol. 2, 2002, pp. 850 –854.

[10] D. Shi, C. Auvigne, R. Besuchet, C. Winter, Y. Civet and Y. Perriard, "Optimal design of inductive coupled power transfer systems with application to electric cars," *2013 Internastional Conference on Electrical Machines and Systems*, Oct. 26-29, 2013, Busan, Korea.

[11] C. Auvigne, P. Germano, D. Ladas and Y. Perriard, "A dual-topology ICPT applied to an electric vehicle battery charger", *XXth International Conference onElectrical Machines (ICEM)*, 2012, pp. 2287-2292,

[12] C. Auvigne, P. Germano, Y. Perriard and D. Ladas, "About Tuning Capacitors in Inductive Coupled Power Transfer Systems," *15th European Conference on Power Electronics and Applications*, 2013, pp.1-10.

[13] C. Auvigne, "Electrical and Magnetical Modeling of Inductive Coupled Power Transfer Systems," PhD Thesis no. 6593, Ecole Polytechnique Fédérale de Lausanne, Switzerland, 2015.

Paolo Germano was born in Lausanne, Switzerland, in 1966 and is native of Italy and Switzerland. He received the M.Sc. in micro-engineering from the Ecole Polytechnique Federale de Lausanne (EPFL) in 1990. He joined the Laboratory of Electromechanics and Electrical Machines (LEME) in the same year. He is currently senior researcher at the Laboratory of Integrated Actuators (LAI). His activities as project leader are mainly focused on test benches dedicated to the measurement and the analysis of stepping motors, BLDC motors, linear actuators and other devices (tactile watch, piezo-actuators). In the domain of wireless power transmission (WPT), he took part in projects in the biomedical field (implanted device supply, transcutaneous stimulation), in the field of electrical vehicle (direct supply, battery recharge stations and dynamic recharge) as well as various projects related to machine tools and wireless computer peripheral supplies.

Yves Perriard was born in Lausanne in 1965. He received the M. Sc. in Microengineering from the Swiss Federal Institute of Technology - Lausanne (EPFL) in 1989 and the Ph D. degree in 1992. Co-founder of Micro-Beam SA, he was CEO of this company involved in high precision electric drive. Senior lecturer from 1998 and professor since 2003, he is currently director of Laboratory of Integrated Actuators. His research interests are in the field of new actuator design and associated electronic devices. In 2009, he is appointed Vice-Director of the Microengineering Institute in Neuchâtel until 2011. In 2013, the Federal Council has named him in the CTI commission in Bern. In 2014, he is appointed guest professor at Zhejiang University in China.